Nanocomposites Based on LDPE Filled with Carbon Nanotubes Prepared by High Energy Ball Milling and its Potential Anti-Bacterial Activity

E. Benigno[1], M.A. Lorente[2], D. Olmos[2], G. González-Gaitano[3] and J. González-Benito[2]

1Dept. Mechanical Engineering. Universidad Carlos III de Madrid, Madrid, SPAIN

2Dept. Materials Science and Engineering, IQMAAB, Universidad Carlos III de Madrid, Madrid, SPAIN

3Dept. Química, Facultad de Ciencias, Universidad de Navarra, 31080, Pamplona, SPAIN.

Abstract: Low density polyethylene, LDPE, based nanocomposites containing multi-walled carbon nanotubes, MWCNT, were prepared by a two-step process consisting in a pre-mixture using high energy ball milling, HEBM, and subsequent hot pressing. The effects of HEBM and presence of MWCNT on some physical properties of the LDPE based materials and antimicrobial efficiency against *DH5α Escherichia coli* were studied. FTIR revealed the polymer structure did not change in the final materials after the addition of MWCNT. Differential scanning calorimetry showed small differences in the LDPE thermal behavior as a function of the type of material due to small changes in the polymer crystallization. This result was mainly ascribed to the milling process rather than to the incorporation of the MWCNT. The presence of 1% by weight of the nanofiller increased the rigidity and hydrophobicity of the nanocomposites respect to the neat LDPE. This effect was explained considering certain presence of the MWCNT in the surface of the material as the main factor of decreasing the polar contribution to the surface free energy. A correlation between hydrophobicity, biofilm development, shape and size of DH5α *E. coli* was observed, indicating that the presence of MWCNT leads to biocide effect by decreasing cell adhesion and changing its metabolism.

Keywords: LDPE; carbon nanotubes; nanocomposites; biocidal effect.

1. Introduction

Storing and transportation of perishable products (e.g. food and food complements) involve using packing materials capable of offering protection against any physical or chemical alterations arising from the action of different agents, such as bacteria, temperature and gases, which may alter the food properties for final consumption. Although many materials are available, plastics are the most demanded in food packaging industry. In fact, about a 39% of the plastic production is nowadays used in the packaging industry and about a 66% of that is used for food packaging.

Over the last ten years there has been a very active research to find plastics with the features of easy processability, good mechanical performance, resistant to adverse conditions of temperature, humidity, UV-Vis radiation, and good barrier properties to gases. Improvement of these materials in terms of providing them with multi-functionality is then required, for instance having control of moisture and antimicrobial activity[1]. However, with the later function one should be careful since direct application of biocide substances onto the surface of food has limitations due to the fact that some of the active agents may diffuse rapidly into the food [2, 3].

Polymers, such as low density polyethylene (LDPE), are the most commonly used for packaging applications because of their mechanical and barrier properties, proper strength and elongation, low cost and lightness[4, 5]. However, its antibacterial activity is nothing remarkable.

In order to control the growth of undesirable microorganisms on food surfaces, different methods of incorporating antimicrobial agents onto the surface or into the polymer can be used[6].

Two are the main approaches to this purpose: i) adding antibacterial substances able to migrate to the surface in direct contact with food; and ii) modifying the polymer (LDPE) to bestow it with antibacterial properties. The first approach has the risk of undesired food perturbations. In this sense, the addition of nanoparticles with antibacterial properties can be an interesting choice. The nanoscopic character of the filler allows their addition in low proportion yet high enough as to significantly change the properties of the polymer matrix. Research efforts in this area have been mainly focused on the development of composite materials using different kinds of nanoparticles [1-8], among others silver [9,10], zinc oxide[11] and titanium dioxide [12, 13].

Although for some systems the use of nanoparticles has been proven to have good efficiency, as it is the case of silver nanoparticles, other choices can be explored looking for the combination of multiple beneficial responses. In this respect, a good choice can be carbon nanotubes (CNTs) because of its capacity to improve the mechanical properties of polymers in which they can be dispersed. In fact direct contact with aggregates of CNTs has been demonstrated to be fatal for *E. coli*. Some investigations had provided evidence that highly purified single-walled carbon nanotubes (SWNTs) exhibited strong antimicrobial activity. Cell membrane damage resulting from direct contact with SWNT aggregates is the most likely mechanism leading to bacterial cell death. They gave the first evidence that the size (diameter) of carbon nanotubes (CNTs) is a key factor governing their antibacterial effects and that the main CNT-cytotoxicity mechanism is cell membrane damage by direct contact with CNTs[14]. Experiments with well-characterized single-walled carbon nanotubes (SWNTs) demonstrate that these are much more toxic to bacteria than multi-walled carbon nanotubes (MWNTs). In addition to this, gene expression data show that in the presence of both MWNTs and SWNTs, *E. coli*. expresses higher levels of stress-related gene products, with the quantity and magnitude of expression being much higher in the presence of SWNTs[14,15].

Other investigations pointed out the potentiality of CNTs as antimicrobial agents in composite materials. *Xiaoming et al.*[16] followed the work previously done by *Aslan et al.*[18] in which SWCNTs were dispersed in a typical polymer used in bioengineering, poly(lactic-co-glycolic acid) (PLGA), to form thin films. These SWCNT–PLGA films were coated on cover glasses with the weight ratio of SWCNTs to PLGA ranging from 1:7000 to 1:70, effectively decreasing the viability of *E. coli* and S. Epidermidis. Moreover, posterior investigations[17, 18] incorporated SWCNTs into electrospun polysulfone mats and applied them as a conformal coating. The freestanding polymer mats with a low weight percentage of incorporated SWCNTs showed strong antimicrobial activity towards *E. coli*. *Nepal et al.* fabricated a multifunctional biomimetic film composed of SWCNT, DNA and lysozyme, using a layer-by-layer assembly method. This composite film, with a high Young's modulus and controlled morphology, showed excellent long-term antimicrobial activity[19].

However, as a final issue to be considered before preparing a nanocomposite, the processing of the raw materials to achieve a uniform dispersion of the nanoparticles within the polymer matrix is of paramount importance. Three are the main methods to produce polymer nanocomposites[20]: melt compounding, solution blending, and in situ polymerization. However, none of them can ensure a uniform dispersion of the nanoparticles when they show at least sizes lower than 50 nm in one dimension and their content is higher than 5 wt%. As an alternative method, high energy ball milling (HEBM), was proven to be very effective in terms of dispersion in the case of the preparation of thermoplastic nanocomposites[21-27].

In this frame, the aim of the present study was to explore the feasibility of producing antibacterial low density polyethylene (LDPE) films by incorporating multi-walled carbon nanotubes, MWCNT. The physical properties of the nanocomposites in the form of films, as well as their antibacterial activity, were investigated in order to understand the possible mechanisms against the biofilm development of the bacteria DH5α *E. coli*.

2. Materials and Methods

2.1. Materials

Low density polyethylene, LDPE, in the form of pellets was supplied by Sigma-Aldrich (density 0.925 g/cm^3 at 25°C and melting point 116°C). Multi-walled carbon nanotubes, MWCNT, used as a the nanofiller, were also acquired from Sigma-Aldrich (density 2.1 g/cm^3 at 25°C, external diameter between 6 and 9 nm and 5 μm length according to the manufacturer, with a composition in carbon > 95 wt%).

As testing liquids for the contact angle measurements distilled and deionized water, glycerol and diiodomethane were chosen. The Table 1 gathers values of some relevant parameters of the testing liquids.

Liquid	δ (g/cm^3)	γ_d (mN/m)	γ_p (mN/m)	γ_t (mN/m)	Supplier
Water	0.998	21.8	51.0	72.8	Home lab
Glycerol	1.259	37.0	26.4	63.4	Panreac
Diiodomethane	3.220	50.8	0.00	50.8	Sigma-Aldrich

Table 1. Values of densities and contributions to the surface tension of the liquids used to carry out the contact angle measurements.

Where δ is the density of the liquid, γ_d and γ_p the dispersive and polar components of the surface tension of the liquids and γ_t the total surface tension. The values of surface tension were taken from *Ström et al.*[28].

2.2. Sample preparation

All samples were prepared in the form of films by two steps, cryomilling and subsequent hot pressing. To help in the process of cryomilling the LDPE pellets were previously grinded using a MF 10 Basic Microfine Miller. In order to avoid excessive plasticity during the grinding process the LDPE was cooled down using liquid nitrogen. The grinding process was carried out at 1500 rpm yielding the product in the form of flakes. The grinded LDPE without nanotubes was further used as the control sample. Then the LDPE and its mixture with MWCNT were milled by high energy ball milling (HEBM) under cryogenic conditions. A mixing miller RESTCH MM400 was used for this purpose. 15 stainless steel balls of 9 mm diameter and 3 g of samples were introduced in a stainless steel vessel of 50 cm^3. Then, the mixture was milled at 25 Hz for 1 hour using cycles of 5 minutes alternating with 15 min of immersion in liquid nitrogen to attain cryogenic conditions to finally obtain a fine powder.

A Fontijne Press TPB374 machine was used to carry out the hot pressing process of the grinded and milled powders. Polished aluminum plates (12 × 12 mm) covered with anti-adherent Kapton® films to avoid adhesion on the plates were used together with a mask of Kapton® film (10 × 10 mm) as a mold. Enough amount of sample was added and then subjected to the corresponding hot-pressing cycle (Figure 1). Films of about 150 μm of thickness were obtained in all cases (Figure 2). Depending on the processing and composition three types of samples were prepared: a) LDPE only subjected to the grinding process; b) cryomilled LDPE (grinded LDPE subjected to the HEBM process); and c) LDPE/MWCNT composites prepared by HEBM.

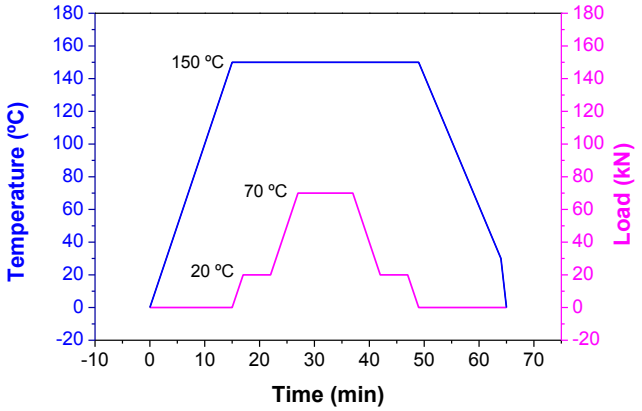

Figure 1. Pressure-Temperature cycle used to perform the hot pressing process.

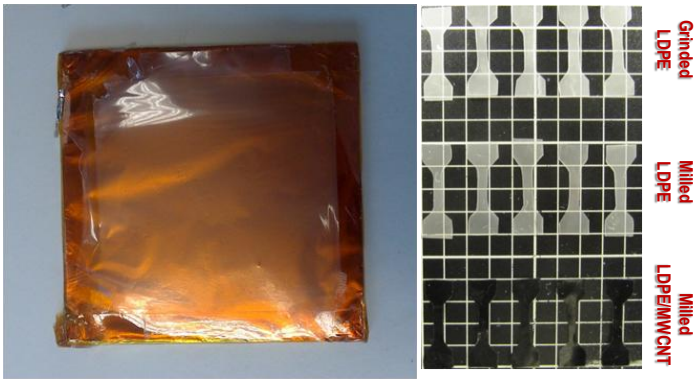

Figure 2. LDPE film obtained from the hot pressing process (left) and specimens of the three types of samples to be used for the stress-strain tests (right).

2.3. Characterization and testing

2.3.1. Attenuated total reflectance FTIR spectroscopy (ATR)

The structure of LDPE has been studied with a Nicolette Avatar 360 Spectrometer, equipped with a Golden-Gate temperature controlled ATR. The spectra were collected with a resolution of 4 cm^{-1} and 32 scans per spectrum, in the range of 600 to 4000 cm^{-1}.

2.3.2. Differential scanning calorimetry, DSC

The possible variations of the thermal behavior of LDPE when milled or modified with MWCNT have been studied using DSC by monitoring the dynamic melting and crystallization processes. The experiments were carried out in a Mettler Toledo 822e Calorimeter under a N_2 atmosphere using samples of ca. 2 mg. In all cases the thermal history was previously erased by heating the samples at 10°C/min from 30°C to 170°C and maintaining the sample at the highest temperature for 10 min. After that, the crystallization process was monitored by cooling down to 30°C at 10°C/min. Finally, the melting process was studied with a second heating cycle from 30°C to 170°C at 10°C/min. Melting, T_m, and crystallization, T_c, temperatures, were obtained from the endothermic and exothermic peaks of the DSC traces, respectively. The crystallization degree, χ, was obtained from the equation 1:

$$\chi \quad \text{———————} \qquad (1)$$

Where X is the weight fraction of the nanofiller (0 for the grinded and milled LDPE, and 0.01 for the LDPE/MWCNT composite), ΔH_m is the fusion enthalpy obtained from the integration of the endothermic peak of the DSC traces, and $\Delta H_m(100\%)=289.9$ J/g is the fusion enthalpy for a 100% crystalline polyethylene sample[29].

2.3.3. Thermogravimetric analysis, TGA

The effects of processing and MWCNT content on the thermos-degradation of LDPE were studied by TGA. The measurements were carried out in a TGA-SDTA 851 Mettler Toledo thermos-balance. Heating ramps from 30°C to 600°C at 10°C/min were carried out under nitrogen atmosphere with a gas flow of 20 ml/min.

2.3.4. Mechanical properties

The films obtained after the hot-pressing process were cut to obtain specimens to carry out stress-strain tests. The dimensions of the specimens followed the ISO standard 3167:2002[30] (Figure 2).

A Shimadzu Autograph Universal Testing Machine was used to perform the tensile tests. Mechanical properties (Young modulus, tensile strength and ductility in terms of maximum deformation at break) were determined from the standard ISO 527-1:1993 and Corrigendum 1:1994. All tests were carried out pulling the specimens with a gauge length of about 28 mm at a crosshead speed of 5 mm/min. Average values of the mechanical properties were obtained from the results of at least five tests corresponding to five specimens.

2.3.5. Contact angle measurements

In order to collect the necessary information to properly interpret bacteria adhesion phenomena, the surface free energy of the different materials was obtained from contact angle measurements. An OCA-15 Plus Goniometer (DataPhysics, Neuterk Instruments, Eibar, Spain) based on the sessile drop method was used according to the EN 828:2009 standard. The contact angle of at least four drops for each testing liquid was measured to finally obtain an average value. The surface free energy was determined using the *Fowkes* method[31, 32].

2.3.6. Scanning electron microscopy, SEM

Biofilms morphologies were inspected with a PHILLIPS XL30 Scanning Electron Microscope using acceleration voltages of 10, 15 and 20 kV. To fix the biofilms and made them conducting the samples were gold coated by a conventional sputtering method. Images from the secondary, SE, and backscattered electrons, BSE, were obtained.

2.3.7. Biofilms preparation

To culture the bacteria DH5α a strain of the bacteria *Escherichia coli* were used. Square pieces of about 8×8 mm of the different materials were cut out and glued with an epoxy adhesive on stainless steel disks. After that the materials were disinfected by spraying with ethanol 70% (v/v). By adding a 3% of *E. coli* to Luria Bertani (LB), used as growth medium, a stock suspension was prepared by culturing it for 12h at 37°C with agitation. Then, a 1/100 dilution of the stock suspension was used as the medium to immerse the three materials and generate the biofilm on their surfaces. Two pieces of each material were treated in order to subsequently perform two different experiments associated to the biofilm development: i) direct observation of bacteria from SEM inspection; and ii) colonies counting from an ulterior culture on agar plate.

To prepare the biofilms a multi-well plate was used introducing one sample per well, and then pouring 2 mL of the diluted suspension into each well. Then, the plate was agitated for 3h at 37°C, waiting the adhesion of bacteria to the surfaces of the materials and so generating the biofilms on them. These conditions were selected after discarding other from preliminary tests. After 3h of culture the suspension was removed by aspiration to eliminate the non-adhered bacteria and the resulting materials rinsed with a sterile solution of sodium chloride 0.9 wt%. The procedure for the cell counting tests was carried out immediately after the biofilms preparation to avoid cellular death and changes in the morphology of the bacteria. The cells adhered to the surfaces of each material (LDPE, milled LDPE and LDPE/MWCNT) were removed using a sterilized cotton swab and transferred into a Falcon tube with 1 mL of LB, leaving it for incubation at 37°C for 1h. After that, an Agar plate was divided into four sections and 10 µL of different dilutions (1/100, 1/1000, 1/10000 and 1/100000) of the initial suspension were zig-zag distributed in each section using an inoculation loop and the plate was cultured at 37°C overnight. Finally, the colonies formed were observed and counted, expressing the results as colony-forming units per milliliter, CFU/mL.

3. Results and Discussion

3.1. Materials characterization

When polymers are modified adding certain fillers they can change its antibacterial activity either by induced structural and morphological variations of the polymer, which might affect the interaction strength between the bacteria and the substrate, or by the direct action exerted on the bacteria by the filler[9-13]. Besides, when a polymer is modified to improve its performance for a specific use it is important to avoid losing other properties such us the mechanical ones, and resistance against thermos-degradation. It is for this reason that a general characterization of the materials was firstly done in order to investigate any possible induced change in the polymers under the presence of the MWCNT. This study can be considered as a previous step to investigate any potential effect in the antibacterial activity of the materials.

The DSC traces corresponding to the first heating and cooling processes, and the second heating are shown in Figure 3.

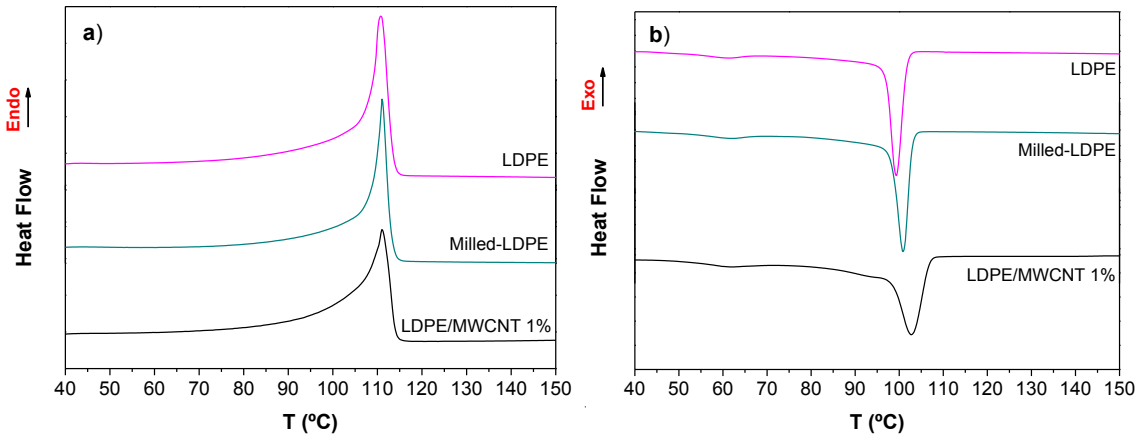

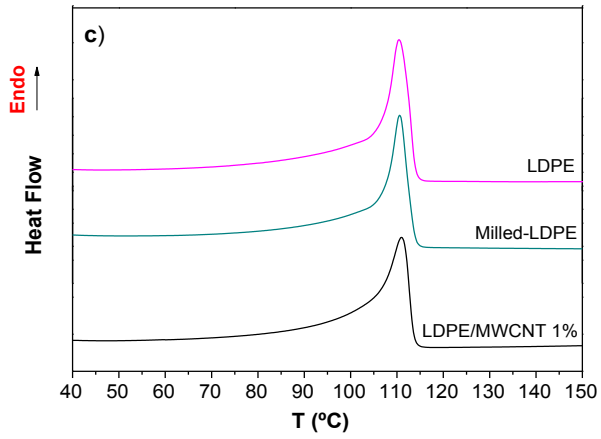

Figure 3. DSC traces corresponding to the first heating (a) and cooling (b) and to the second heating (c).

In the first heating (Figure 3a) it can be observed that the three materials show a similar behavior, with only one endothermic peak centered almost at the same temperature, corresponding to the melting of the LDPE. Only little differences can be observed: the milled LDPE presents the narrowest and sharpest melting peak, while the LDPE/MWCNT nanocomposite the broadest one. The width of the melting peak is usually related with the heterogeneity of the crystals that melt (perfection and size). On the other hand, for the cooling cycle, the milling process does not seem to affect the thermal behavior and only clear differences are observed when MWCNT are incorporated to the LDPE (Figure 3b), as the exothermic peak broadens and the crystallization temperature at the minimum slightly increases from 100°C for the pure LDPE to 102°C for the nanocomposite. The former observation can be attributed to a more heterogeneous crystallization while the latter is usually indicative of a nucleating effect, making the crystallization process to start earlier. Crystallization occurs at ~100 ºC what agrees with previous studies[12,33,34]. The presence of the secondary peak at lower temperatures has been attributed to a thermal relaxation process although its microscopic origin is still unclear. During the second heating scan, after erasing the thermal history, the materials do not show clear differences; just a slightly broader endothermic peak was obtained for the nanocomposite (Figure 3c).

The crystalline fraction, χ, in each system was calculated from the integration of the endothermic and exothermic peaks using the following expression:

$$\chi = \frac{\overline{\qquad}}{\qquad} \quad (1)$$

Where ΔH_m and ΔH_c are the enthalpies of fusion and crystallization, respectively, x is the weight fraction of MWCNT, and ΔH_m^0 is the enthalpy of fusion for the fully crystallized polyethylene, $\Delta H_m^0 = 289.9$ J/g[29]. The values obtained for the crystalline fraction were 0.41, 0.36 and 0.37 for LDPE, milled-LDPE and LDPE/MWCNT, respectively. These results point out that more than the sole incorporation of MWCNT the milling process seems to be the main cause of the changes observed. Therefore, when comparing "milled LDPE" and "LDPE/MWCNT" in terms of crystallinity if any property change is observed it must be due to the presence of MWCNT rather than to variations in the polymer structure and morphology.

In Figure 4 the thermogravimetric curves of the materials under study and their derivatives are shown in order to see possible variations in the thermos-degradation process under the influence of the milling and the presence of MWCNT.

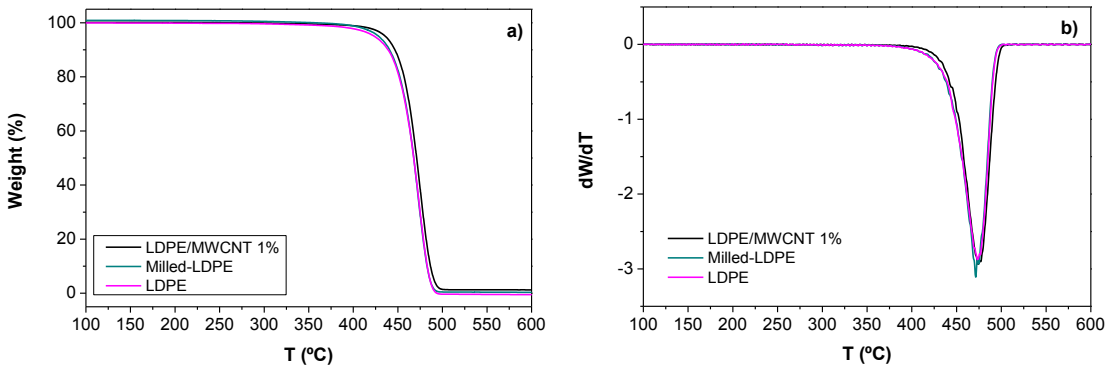

Figure 4. Thermogravimetric analysis (a) and derivative (b) curves of the different LDPE based films.

It cannot be observed any significant difference between the results obtained for the three systems, but only a very small shift to higher temperatures in the case of the nanocomposite film. It seems therefore that neither the milling nor the incorporation of 1% of MWCNT affects the thermos-degradation process of the LDPE, concluding that there are no structural changes in the polymer due, for instance, to oxidation processes or bonds scission by mechanical activation promoted by the HEBM and favored by the presence of MWCNTs. However, in the case they existed it should be possible to observe those changes in the infrared spectrum.

The ATR-FTIR spectra of the different samples are shown in Figure 5. In all cases the typical absorption bands of polyethylene[33] can be observed at 2916, 2847, 1460 and 725 cm^{-1} respectively, with the lack of changes in the relative absorbance and in the shape of the bands, confirming the absence of structural changes in LDPE due to either the HEBM process or the presence of 1% of MWCNTs.

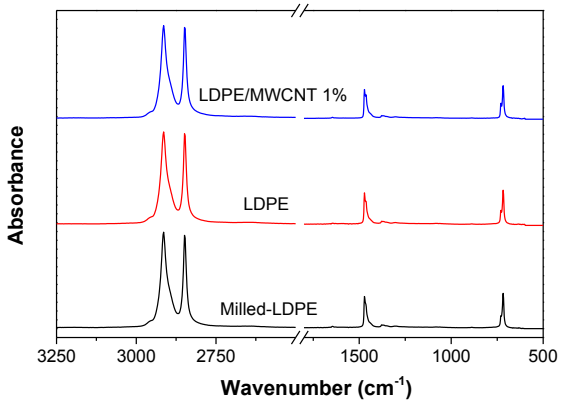

Figure 5. ATR-FTIR spectra of the different LDPE based films.

So far, and in terms of characterization, when comparing between the three materials considered, only a small change has been found, i.e., the crystallinity degree, which depends on the milling and that might have consequences in the mechanical properties of the material.

Three representative stress-strain curves of the different films are shown in Figure 6. All of them show the typical profile of tensile test curves of semi-crystalline polymers.

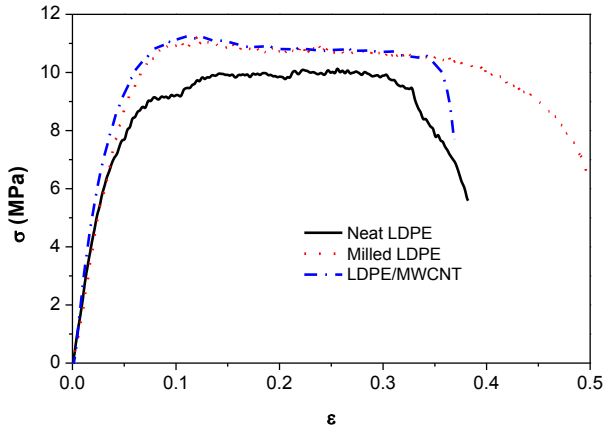

Figure 6. Representative stress-strain curves of the materials under study.

By overlapping the three representative curves it is observed that the material does not change in terms of mechanical performance after milling. Only when MWCNT are added the material behaves with slightly more rigidity (see Table 2, where data of the mechanical parameters are gathered). In particular, all the data remain nearly constant except the Young's modulus, which increases over 10% when 1 wt% of MWCNT is added. This result is completely in accordance with results found in the literature[35] and confirms that addition of small amount of MWCNT increases certain mechanical properties. These slight variations in mechanical properties might be attributed mainly to the addition of the filler, as no significant changes in the degree of crystallinity were observed between milled LDPE and LDPE/MWCNT.

Sample	Tension strength (MPa)	Young's Modulus (MPa)	Deformation
LDPE	10.1 ± 0.2	230 ± 71	0.53 ± 0.13
Milled LDPE	11.4 ± 0.2	232 ± 12	0.52 ± 0.15
LDPE/MWCNT	11.2 ± 0.3	299 ± 17	0.51 ± 0.17

Table 2. Data corresponding to the mechanical parameters extracted from the stress-strain curves.

To obtain the surface free energy, contact angle measurements were carried out. The corresponding values are gathered in Table 3.

	Contact Angle (º)		
Sample	Water	Glycerol	Diiodomethane
LDPE	99	103	62
Milled LDPE	100	87	65
LDPE/MWCNT	117	96	65

Table 3. Values of contact angle obtained for the three test liquids used.

When water is used as the test liquid it is observed an increase of about 18% in the contact angle for the nanocomposite with 1 wt% of MWCNT, indicating that a more hydrophobic surface is generated. Taking into account that significant structural changes were not observed by FTIR between the samples and that the small changes in the degree of crystallinity seem to be mainly due to the milling process, it should be conclude that the differences in the contact angle must come from other causes. A possible explanation can be the presence of a certain amount of MWCNT on the surface of the nanocomposites. Although the content of MWCNT is quite low, 1 wt%, their surface to volume ratio is extremely high so their contribution to the total surface exposed to a water droplet can be high enough as to exert some influence on the water adhesion.

To obtain the surface free energy as well as their polar and dispersion contributions the Fowkes method was used[31, 32]. The values of these parameters can be found in the Table 4.

Sample	Surface Free Energy (mN/m)	Polar part (mN/m)	Dispersive part (mN/m)
LDPE	28.4	1.0	27.4
Milled LDPE	26.7	1.0	25.7
LDPE/MWCNT	25.9	0.2	25.7

Table 4. Values of surface free energy obtained from the use of the Fowkes method.

The usual values of surface free energy found in the literature for the LDPE are in the range 25-40 mN/m, with a polar contribution ranging from 0.7 mN/m to 4 mN/m[36], which are similar to the experimental data obtained in the present work (Table 4).

According to the data of the Table 4, a slight decrease (~6%) in the surface free energy is observed after milling, associated to a decrease in the dispersive contribution. A possible cause can be the decrease in the crystallinity degree. It is known that the crystallinity degree, clearly influences the surface free energy, being able to change almost in a 50% from 0% to 100% of crystallinity degree in the polyethylene[37, 38]. When MWCNT are introduced the surface free energy of the hot pressed films decreased slightly more (~9%). In this case, there is again a diminution in the dispersive contribution to the surface free energy, but also there is a decrease in the polar contribution. Since the former effect can be associated to the decrease in the degree of crystallinity, the latter should be ascribed to the presence of MWCNT. As it was mentioned above, MWCNT can form part of the nanocomposite surface, therefore a reduction of the polar traces appearing in the neat polyethylene is expected.

3.2. Biofilm development and microbiology analysis

In order to compare biofilm development as a function of the type of material, SEM images were taken at different magnifications using both the signal coming from secondary electrons, SE, and backscattered electrons, BSE. With the later signal, information from compositional distribution can also be visualized.

SEM images (SE signal) of the biofilms formed on the surfaces of the three materials under study are shown in Figure 7. At lower magnification it is clearly seen how there is a larger surface of material covered by biofilm when the neat LDPE is used. On the other hand, when comparing the milled LDPE with the nanocomposite LDPE/MWCNT (Figures 7c and 7e) the difference is not so clear. In fact it seems that the differences follow similar trends to the crystallinity degree and surface free energy, which suggest a certain correlation between biofilm development and crystallinity degree and surface free energy. At higher magnification, by choosing regions where there is high concentration of bacteria (Figures 7b, d and f), no so clear differences are observed. Due to this, a deeper observation using the BSE signal was used.

SEM images (BSE signal) of biofilms formed on the surfaces of the three materials under study are shown in Figure 8. In all cases cylindrical shape microorganisms are observed surrounded by a halo characterized by a higher brightness (higher BSE intensity). This observation is informing us about a substance composed by heavier elements, as can be those coming from salts that form part of the polymeric extracellular substance that bacteria used as food and to be attached to the substrate surface. In Figure 9 a zoomed view of the images of Figure 8 is presented. Seemingly, the size and shape differ depending on the substrates to which the bacteria are attached.

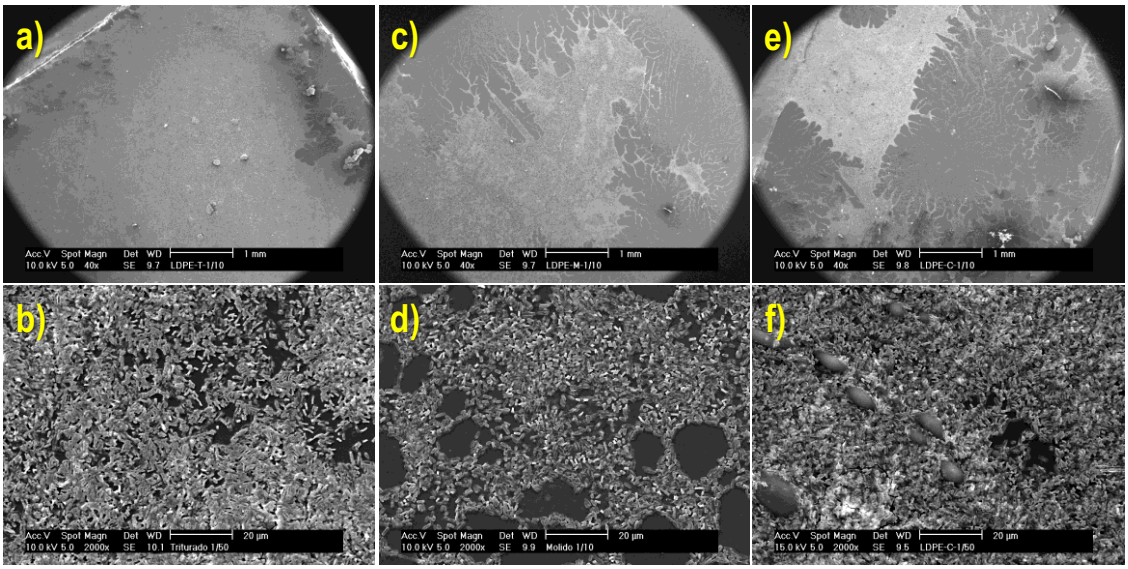

Figure 7. SEM images (SE signal) of biofilms formed on the surfaces of the three materials under study.

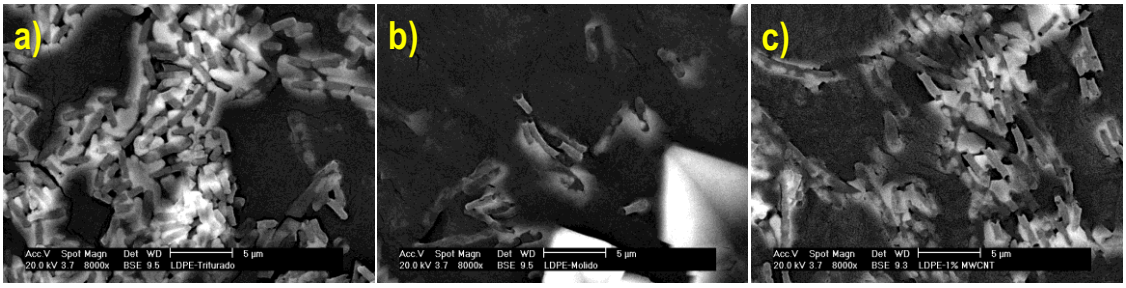

Figure 8. SEM images (BSE signal) of biofilms formed on the surfaces of the three materials under study

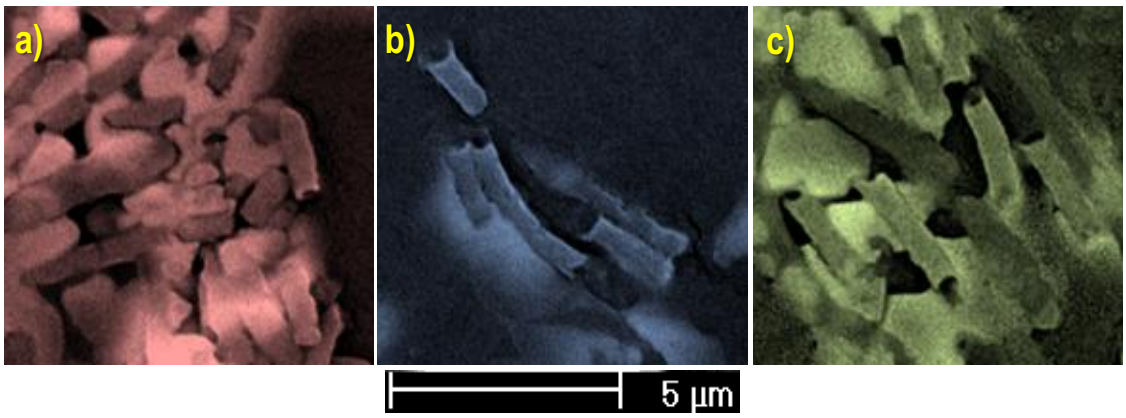

Figure 9. Zoomed view of the micrographs of Figure 8: a) LDPE; b) Milled LDPE and c) MWCNT-LDPE

For the LDPE E. Coli seems to be developed with obloid shape, while in the cases of milled LDPE and LDPE/MWCNT composite bacteria are more cylindrical and with slightly higher sizes. To corroborate this last observation, some detailed measurements of the bacteria size were performed, taking at least 10 cells. The resulting dimensions are collected in Table 5. As can be seen, there is a correlation between the tendencies in terms of size and the biofilm development, i.e., the higher the amount of bacteria and extracellular polymeric substance the smaller the bacteria.

Substrate	Height (μm)	Width (μm)
LDPE	1.7± 0.2	0.58 ± 0.05
Milled LDPE	1.8± 0.1	0.57 ± 0.03
LDPE/MWCNT	2.6 ± 0.2	0.62 ± 0.03

Table 5. Data about bacteria dimensions developed on the three substrates studied.

These results suggest that the substrate not only affects the adhesion of E. coli and the EPS, but also somehow on the metabolism of the cells: with a lower adhesion between E. coli and the surface of the LDPE/MWCNT substrate, the cells are expanded or stressed what should influence in the subsequent live behavior.

To confirm the study done by microscopy experiments of counting bacteria colonies were carried out. Figure 10 shows the colonies of E. coli DH5α obtained by following the process described in the experimental part in the three materials studied.

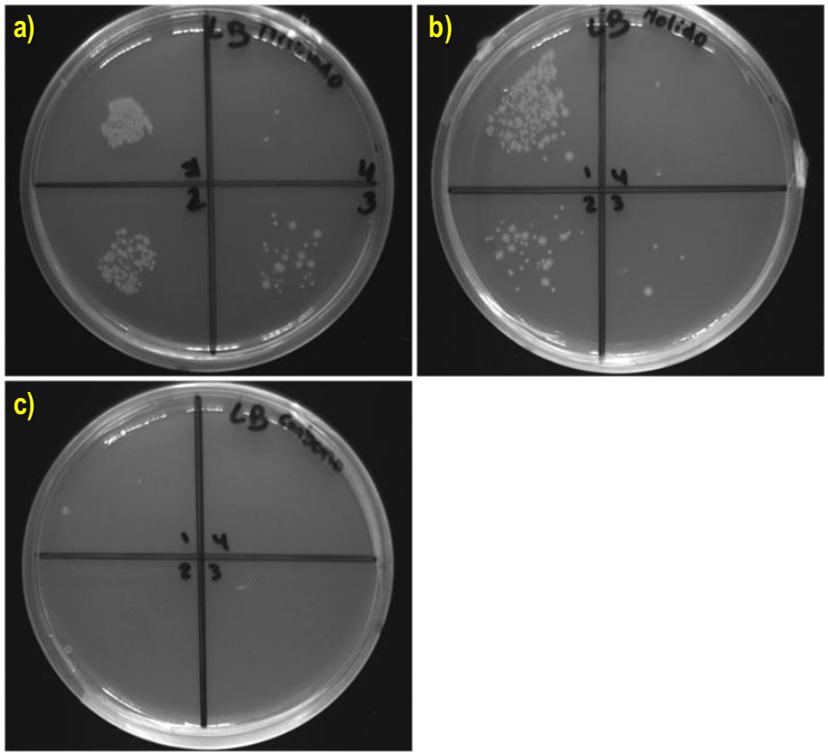

Figure 10. Colonies obtained colonies of DH5α bacteria obtained from the biofilms generated on the surfaces of the materials studied.

Comparing the three samples it can be clearly observed how the number of colonies decreases in the order LDPE > milled LDPE > LDPE/MWCNT nanocomposite. Therefore, we can conclude that the milling process somehow inhibits the DH5α biofilm development and this effect is even higher when 1% of MWCNT are incorporated within the LDPE. The average number of colonies counted in the third quadrant was used to finally obtain the quantitative value of CFU/mL: 2.6×10^7 CFU/mL for the inoculate coming from the biofilm on the LDPE; 4.0×10^6 CFU/mL for the inoculate coming from the biofilm on the milled LDPE and 0.0 CFU/mL for the inoculate coming from the biofilm on the LDPE/MWCNT nanocomposite.

These results point out that, after processing the LDPE by HEBM under cryogenic conditions, it acquires certain biocide character at least in comparison with the commercial LDPE. If

additionally 1 wt% of MWCNT is incorporated to the polymer using the same processing method the antibacterial effect is further increased. A possible explanation is that the biofilm development depends on the adhesion ability of E. coli to the surface of the materials.

Taking into account the results coming from the contact angle measurements (Tables 3 and 4) one can perceive that there is a correlation between surface free energy, the polar character of the surface and the antibacterial character of the materials under study. In fact, the lower the surface free energy, the higher the biocide character; being even higher the lower the polarity of the surface.

5. Conclusions

In this work biocide action of materials based in LDPE filled with MWCNT was investigated. In particular, the effect of processing and the presence of the nanotubes were both analyzed in depth to understand the major causes that may lead to the inhibition of bacterial growth and biofilm formation on the surface of these materials. Firstly, a general characterization of the materials under study (LDPE, milled LDPE and milled LDPE-MWCNTs) was carried out. In general terms, no significant changes were observed by FTIR spectroscopy, but just slight differences in the degree of crystallinity, mainly induced by the milling process. In terms of thermal degradation of the materials, TGA, there were no evidences of structural changes such as oxidation or chain scission. As expected, the mechanical behavior of the samples showed variations in rigidity when MWCNTs were present. On the other hand, HEBM as well as the presence of MWCNTs did produce changes in the surface properties of the material. In fact, surface energy of LDPE decreases with milling and it decreases even more when nanotubes are present. Studies on biofilm development and microbiological analysis of the samples showed that after processing the LDPE by HEBM under cryogenic conditions it presented a certain biocide character in comparison with the commercial LDPE. When 1% of MWCNT is added to the polymer using again the HEBM method the antibacterial action increases even more. Our results suggest that biofilm development depends strongly on the adhesion of *E. coli* to the surface of the materials, so that, the lower the surface energy the more important the effect on the antibacterial action of the material. Although further experiments will be carried out to investigate in depth these trends.

Acknowledgments: Authors gratefully acknowledge financial support from the projects MAT2010-16815 (Ministerio de Ciencia e Innovación), MAT2014-59116-C2-1-R (Ministerio de Economía y competitividad), and CROWDFUNDING (Ref.: 2015/00486/001, Title: Prevención de enfermedades con Materiales Antimicrobianos en los sectores de alimentación y Sanitario).

References

1. Alonso-Calleja, C.; Guerrero-Ramos, E.; Alonso-Hernando, A.; Capita, R. *Food Control*. **56**: 86–94 (2015).
2. Ortega Morente, E.; Fernández-Fuentes, M.A.; Grande Burgos, M.J. et al. *Int. J. Food Microbiol*. **162:** 13–25 (2013).
3. Duncan, TV. *J. Colloid Interface Sci.* **363**: 1–24 (2011).
4. Kormin, S.; Kormin, F.; Beg, M.D.H.; Piah, M.B.M. *IOP Conf. Ser. Mater. Sci. Eng.* **226:** UNSP 012157 (2017).
5. Goyal, M.; Goyal, N.; Kaur, H. et al. *Perspec. in Sci.* **8**: 403-405 (2016).
6. Sung, S.Y.; Sin, L.T.; Tee, T.T. et al. *Trends Food Sci. Technol*. **33**: 110–123 (2013).
7. Palza, H. *Int. J. Mol. Sci.* **16**: 2099–2116 (2015).
8. Malekkhaiat-Häffner, S.; Malmsten, M. *Adv. Colloid Interface Sci.* **248**: 105–128 (2017).
9. Franci, G.; Falanga, A.; Galdiero, S. et al. *Molecules*. **20**: 8856–8874 (2015).
10. Kasraei, S.; Sami, L.; Hendi, S. et al. *Restor. Dent. Endod.* **39**: 109–14 (2014).
11. Sirelkhatim, A.; Mahmud, S.; Seeni, A. et al. *Nano-Micro. Lett.* **7**: 219–242 (2015).
12. Arroyo, J.M.; Olmos, D.; Orgaz, B.; Puga, C.H.; San José, C.; González-Benito, *J. RSC Adv.* **4:** 51451–51458 (2014).
13. Nieto Pozo, I.; Olmos, D.; Orgaz, B.; Božanić, D.K.; González-Benito, *J. Mater. Lett.* **127**: 1–3 (2014).
14. Lukowiak, A.; Kedziora, A.; Strek, W. *Adv. Colloid Interface Sci.* **236**: 101–112 (2016).
15. Yousefi, M.; Dadashpour, M.; Hejazi, M. et al. *Mater. Sci. Eng. C.* **74**: 568–581 (2017).
16. Li, X.; Liu, X.; Huang, J. et al. *Surf. Coatings Technol*. **206**: 759–766 (2011).
17. Aslan, S.; Zoican Loebick, C.; Kang, S.; Elimelech, M.; Pfefferle, L.D.; Van Tassel, P.R. *Nanoscale* **2**: 1789–1794 (2010).
18. Wang, G.; Yu, D.; Kelkar, A.D.; Zhang, L. *Prog. Polym. Sci.* **75**: 73–107 (2017).
19. Li, P.; Liu, D.; Zhu, B. et al. *Compos. Part A. Appl. Sci. Manuf.* **68**: 72–80 (2015).
20. Yilmaz, G.; Ellingham, T.; Turng, L.S. *Polymers (Basel)*. 10 (2017).
21. Castrillo, P.D.; Olmos, D.; Amador, D.R.; González-Benito, J. *J. Colloid Interface Sci.* **308**: 318–324 (2007).
22. González-Benito, J.; Castillo, E.; Caldito, J.F. *Eur. Polym. J.* **49**: 1747–1752 (2013).
23. Olmos, D.; Martínez-Tarifa, J.M.; González-Gaitano, G.; González-Benito, *J. Polym. Test.* **31:** 1121–1130 (2012).
24. Sánchez, F.A.; Redondo, M.; González-Benito, J. *J. Appl. Polym. Sci.* **132**: 41497 (2015).
25. Delogu, F.; Gorrasi, G.; Sorrentino, A. *Prog. Mater. Sci.* **86**: 75–126 (2017).
26. Yang, G.; Li, X.; He, Y. et al. *Prog. Polym. Sci.* **81**: 80–113 (2018).
27. Gorrasi, G.; Sarno, M. et al. *J. Polym. Sci. Part B: Polym. Phys*. **45**: 1390-1398 (2007)
28. Ström, G; Fredriksson, M. et al. *J. Coll. Interface Sci.* **134**: 107–116 (1990).
29. Mandelkern, L. *Crystallization of Polymers in Equilibrium Concepts*, 2nd ed. Cambridge University Press, New York, (2011).
30. Sanchez, F.A.; González-Benito, J. *Polym. Compos.* **38**: 277-235 (2017).
31. Fowkes, F.M. *Ind. Eng. Chem.* **56**: 40–52 (1964).
32. Fowkes, F.M. *J. Adhes.* **4**: 155–159 (1972).
33. Gonzalez-Benito, J.; González-Gaitano, G.; Olmos, D. *RSC Adv.* **5**, 34979–34984 (2015).
34. González-Gaitano, G.; Pontes-Quero, G.; Gonzalez-Benito, J.; Corral, A.; Olmos, D.; *Nanomaterials.* **8(2)**: 60 (2018)
35. Zare, Y. *Synthetic Metals.* **202**: 68-72 (2015).
36. Novak, I.; Steviar, M.; Popelka, A. et al. *Polymer Engineering and Science*. **53**: 516-523 (2013).
37. Kim, K.S.; Park, C.S. et al. *Polymer*. **44**: 6287-6295 (2003).
38. van Krevelen, D.W.; Nijenhuis, K. *Properties of Polymers: Their Correlation with Chemical Structure; their Numerical stimation and Prediction from Additive Group Contributions*. 4th ed. Elsevier, The Neederlands (2009**).**

Tables

Liquid	δ (g/cm^3)	γ_d (mN/m)	γ_p (mN/m)	γ_t (mN/m)	Supplier
Water	0.998	21.8	51.0	72.8	Home lab
Glycerol	1.259	37.0	26.4	63.4	Panreac
Diiodomethane	3.220	50.8	0.00	50.8	Sigma-Aldrich

Table 6. Values of densities and contributions to the surface tension of the liquids used to carry out the contact angle measurements.

Sample	Tension strength (MPa)	Young's Modulus (MPa)	Deformation
LDPE	10.1 ± 0.2	230 ± 71	0.53 ± 0.13
Milled LDPE	11.4 ± 0.2	232 ± 12	0.52 ± 0.15
LDPE/MWCNT	11.2 ± 0.3	299 ± 17	0.51 ± 0.17

Table 7. Data corresponding to the mechanical parameters extracted from the stress-strain curves.

	Contact Angle (º)		
Sample	Water	Glycerol	Diiodomethane
LDPE	99	103	62
Milled LDPE	100	87	65
LDPE/MWCNT	117	96	65

Table 8. Values of contact angle obtained for the three test liquids used.

Sample	Surface Free Energy (mN/m)	Polar part (mN/m)	Dispersive part (mN/m)
LDPE	28.4	1.0	27.4
Milled LDPE	26.7	1.0	25.7
LDPE/MWCNT	25.9	0.2	25.7

Table 9. Values of surface free energy obtained from the use of the Fowkes method.

Substrate	Height (μm)	Width (μm)
LDPE	1.7± 0.2	0.58 ± 0.05
Milled LDPE	1.8± 0.1	0.57 ± 0.03
LDPE/MWCNT	2.6 ± 0.2	0.62 ± 0.03

Table 10. Data about bacteria dimensions developed on the three substrates studied.

Figures

Figure 1. Pressure-Temperature cycle used to perform the hot pressing process. 4
Figure 2. LDPE film obtained from the hot pressing process (left) and specimens of the three types of samples to be used for the stress-strain tests (right). 4
Figure 3. DSC traces corresponding to the first heating (a) and cooling (b) and to the second heating (c). 7
Figure 4. Thermogravimetric analysis (a) and derivative (b) curves of the different LDPE based films. 8
Figure 5. ATR-FTIR spectra of the different LDPE based films. 8
Figure 6. Representative stress-strain curves of the materials under study. 9
Figure 7. SEM images (SE signal) of biofilms formed on the surfaces of the three materials under study. 11
Figure 8. SEM images (BSE signal) of biofilms formed on the surfaces of the three materials under study 11
Figure 9. Zoomed view of the micrographs of Figure 8: a) LDPE; b) Milled LDPE and c) MWCNT-LDPE 11
Figure 10. Colonies obtained colonies of DH5α bacteria obtained from the biofilms generated on the surfaces of the materials studied. 12